SIN-CHN
SCIENTIFIC PRESS PTE.LTD.

Molecular & Cellular Biomechanics 2025, 22(3), 934.
https://doi.org/10.62617/mcb934

Article

Immune and metabolic pathways of microbial population structure remodeling in biopharmaceuticals for intestinal diseases

Jun Yan

School of Nursing and Health Management, Wuhan Donghu University, Wuhan 430212, China; Isabella267738@163.com

CITATION

Yan J. Immune and metabolic pathways of microbial population structure remodeling in biopharmaceuticals for intestinal diseases. Molecular & Cellular Biomechanics. 2025; 22(3): 934. https://doi.org/10.62617/mcb934

ARTICLE INFO

Received: 27 November 2024
Accepted: 9 December 2024
Available online: 13 February 2025

Abstract: Gut microorganisms have become a hot spot of scientific research at home and abroad in recent years, in which the study of correlation between microbial community structure and intestinal diseases can provide theoretical basis for biopharmaceuticals for intestinal diseases. In this paper, we constructed in vitro simulated gastric and small intestinal digestion models, as well as large intestinal microbial fermentation models, to study the relative molecular weight and spatial structure changes of *β*-glucan in simulated gastric and small intestinal regions, and investigated the degradation of *β*-glucan in simulated large intestinal regions as well as its effects on intestinal microorganisms. In addition to the biochemical and metabolic aspects, integrating biomechanical principles into this research can enhance our understanding of how gut microbes interact with the host's physiological environment. For instance, the biomechanical properties of the gut—such as motility, peristalsis, and the mechanical forces exerted on microbial populations—can influence the distribution and activity of gut microorganisms. Understanding these biomechanical factors may reveal how they affect the degradation of β-glucan and the overall microbial community structure. Secondly, fecal microorganisms from different batches of mice and different individuals of human volunteers were collected as inoculum for fermentation of *β*-glucan, to analyze the main microorganisms that stably responded to *β*-glucan in different batches of fermentation experiments as well as in gut microorganisms from different individuals and to further investigate the metabolic changes, metabolic pathways as well as the biomarkers of *β*-glucan in the simulated large intestine. *L. murinus Mic06*, *L. murinus Mic07*, *L. murinus Mic08*, and *L. murinus Mic094* were validated to be able to utilize *β*-glucan and produce a small amount of reducing sugars in all four species of Lactobacillus intestinalis in mice, and there was no significant difference in the ability to utilize them; All nine species of human enterobacteriophages were able to utilize *β*-glucan and produce reducing sugars, with *B. xylanisolvens Bac02* and *B. koreensis Bac08* having a significantly greater ability to utilize *β*-glucan. This study contributes to a deeper understanding of gut disease-associated flora and provides strong support for the use of the gut microbiome for multidisease classification. Additionally, considering biomechanical aspects may lead to novel insights into the interactions between gut microbes and host physiology, enhancing the development of targeted biopharmaceuticals.

Keywords: gut microbes; community structure; intestinal diseases; *β*-glucan; biomarkers; biomechanics; gut motility; microbial interactions

1. Introduction

Intestinal flora mainly exists in the lower gastrointestinal tract colon and rectum, especially the lower gastrointestinal tract has the closest relationship with intestinal flora, and almost all gastrointestinal diseases are associated with intestinal flora. In recent years, more and more studies have focused on the influence of the interaction between intestinal flora and drugs in the treatment of intestinal diseases.

Drug metabolism and therapeutic efficacy depend not only on the organism itself, but also on the micro-ecosystem present in the gastrointestinal tract of the host [1,2]. The intestinal tract is the main site of drug absorption, and the intestinal flora directly or indirectly affects the metabolism of various drugs, and at the same time, drugs also affect the composition and function of the intestinal flora, and the two form a potential interaction mechanism [3–6]. Some researchers have even given a new term to this mechanism, i.e., pharmaco-microbiomics. Studies have shown that a diversity of biotransformation reactions exists in the human gut that are dominated by reduction and hydrolysis reactions and supplemented by oxidation, hydroxylation, dehydroxylation, dealkylation, deamination, deacetylation, acetylation, and deacetylation reaction types [7–10]. Whereas, biotransformation reactions in the form of microbial enzyme catalysis directly alter the efficacy and toxicity of drugs by activating, deactivating and regulating drug metabolism [11,12]. Gut microbes can also indirectly control drug efficacy and toxicity by altering host metabolism and producing metabolites that compete with drug receptors. In turn, the composition of the gut flora can vary depending on the amount and combination of ingested drugs [13–15]. Drug-induced changes in the intestinal flora may alter the concomitant pharmacokinetics of the drug [16,17]. Significant differences in the composition of the flora were observed in patients taking a single drug for a long period of time compared to non-drug taking patients [18]. Therefore, studying the structural remodeling of the microbial community is crucial for the treatment of intestinal diseases.

In conclusion, although many studies have confirmed the correlation between the intestinal flora and various diseases, most intestinal bacteria are not able to develop the problem in vitro, and become a bottleneck in the study of the mechanism of intestinal flora and disease. In addition, the intestinal flora were in dynamic changes, and the study of disease specificity, disease diagnosis, treatment and prediction was increased.

In this paper, an in vitro gastrointestinal digestion model was first constructed to analyze the gastrointestinal digestive properties of *β*-glucan, and the effect of gastric acid on the physicochemical properties of *β*-glucan was proposed and verified. Subsequently, an in vitro intestinal fermentation model was constructed to simultaneously examine the roles of human and mouse intestinal microorganisms in the intestinal metabolism of *β*-glucan, as well as the metabolic changes and metabolites of *β*-glucan. Next, microorganisms in the gut capable of utilizing *β*-glucan were specifically screened and their ability to metabolize *β*-glucan was verified. Further, intestinal microorganisms with strong metabolizing ability for *β*-glucan were selected to reveal their metabolizing mechanism for *β*-glucan from the perspective of genome and carbohydrate-active enzymes. Meanwhile, the biosynthetic pathway from *β*-glucan to SCFAs was analyzed and the effect of polysaccharide structure on metabolite synthesis was elucidated. Finally, the effects of *β*-glucan intestinal metabolism on intestinal health are explored by cellular and animal experiments.

2. Materials and methods

2.1. Purpose of the experiment

Digestion and absorption of dietary polysaccharides in humans may involve three

different ways [19]:

(1) Direct digestion and absorption.

(2) Direct absorption through endocytosis.

(3) Degradation and further metabolism by intestinal microorganisms. Polysaccharides that can be directly digested and absorbed by humans usually include starch and dextrins, while most other non-starch polysaccharides are mainly fermented and degraded by intestinal microorganisms in the large intestine due to the limited ability of humans to synthesize their own glycan-degrading enzymes. Prebiotic strains (β-glucan) are a type of non-starch polysaccharide, however there is currently controversy regarding the digestion and degradation of prebiotic strains in the gastrointestinal tract. On the one hand, probiotic strains can be partially degraded in the stomach and small intestine [20]. On the other hand, probiotic strains are not digested in the gastric and small intestinal environments, but are fermented by human gut microorganisms and then degraded and utilized [21]. Therefore, more studies are needed to elucidate the metabolism of probiotic strains in the stomach, small intestine and large intestine.

Based on this, the present study was conducted by simulating gastrointestinal digestion in vitro in order to study the changes of probiotic strains in the stomach and small intestine, and by simulating gastric acid conditions alone in order to examine whether the changes of probiotic strains in the simulated stomach and small intestine were due to the effect of gastric acid. Then, mouse and human fecal microorganisms were inoculated simultaneously for in vitro simulated intestinal fermentation in order to study the catabolism of probiotic strains in the presence of intestinal microorganisms and the effect of probiotic strains' external fermentation on intestinal microorganisms in the hope of providing basic understanding of metabolic processes of probiotic strains in the organism, as well as providing a reference to explore the bio-pharmaceuticals for intestinal diseases.

2.2. Experimental materials and equipment

2.2.1. Equipment and instruments

The equipment and apparatus used in the experiment are shown in **Table 1**.

Table 1. Equipment and instruments required for model construction and behavior experiment.

Instruments and equipment	Corporation
Oaks electric hair shaver	Oaks Appliance Store
Electrical stimulator for experiments	Self-control
Touch TestR	North Coast
Noldus behavior analysis system	Noldus, Netherlands
YB electronic balance, model 1201	Shanghai Haikang electronic instrument factory
Medical suture needle	Smith Barney Medical Devices
DK-S24 type electric thermostatic water bath	Shanghai Senxin Experimental Instrument Co., LTD
Open field experiment	Self-control
IMS-30 ice machine	Huayu Brothers refrigeration equipment Co., LTD

Table 1. (*Continued*).

Instruments and equipment	Corporation
DW-86L338J ultra-low temperature refrigerator	Haier special electric flagship store
Mettler Toledo electronic balance	Mettler Toledo Instruments (Shanghai) Co., LTD
Independent air supply isolation cage IVC-II	Feng experimental animal equipment Co., LTD

2.2.2. Drugs and reagents

The drugs and reagents used in the experiment are shown in **Table 2**.

Table 2. Pharmaceutical reagents required for model construction and behavioral experiments.

Reagents and drugs	Corporation
Anhydrous ethanol (analytical pure)	Sinopharm Group Chemical reagent Co., LTD
Cane sugar	Sinopharm Group Chemical reagent Co., LTD
Pentobarbital sodium	Soleibao Biotechnology Co., LTD
Povidone iodine solution	Minsheng Pharmaceutical Co., LTD
Sodium chloride injection	Shunhong Veterinary Drug Co., LTD

2.2.3. The establishment of the external simulation model

The comparison of Cefonii, physiological salt water, antibiotics and probiotics (the specific content of the experimental design) and 30 mL of simulated gastric juice were mixed. In this paper, the gastric fluid was mixed with the simulated gastric electrolyte. Using HCL solution to adjust the pH to 2.0 and incubation for 1–4 h water bath in 37 ℃. After the end of each time period, the simulated fluid of 20 mL of digestion was treated with an inenzymase processing, 5000 r/min centrifuges, 10 min, and collected the liquid and 20 ℃.

After the gastric digestion, the simulated liquid was mixed with 30 mL, and the solution of the solution pH was 7.0, and incubation in 37 ℃ water bath. After the end of each time period, the simulated fluid of 20 ml of digestion was treated with an inenzymase processing, 5000 r/min centrifuges, 10 min, and collected the liquid and 20 ℃.

2.3. Experimental design

The experimental design process was as follows, 40 SD rats were acclimatized for one week before the start of the formal experiment, after which they were divided into four groups ($N = 10$), which were blank control group (Ctrl), model group (AB-Ctrl), probiotic intervention group 1 (AB-Prob) and probiotic intervention group 2 (AB + Prob).

(1) The blank control group was gavaged with saline for 3 weeks of the experiment.

(2) The model group was gavaged with cefdinir in the first week and saline in the second 2 weeks.

(3) Probiotic intervention group 1 was gavaged with probiotic solution for 2 weeks after one week of cefdinir.

(4) Probiotic intervention group 2 was gavaged with both antibiotics and probiotics in the first week (gavage of cefdinir followed by probiotics at 4–5h intervals), and then continued to be gavaged with probiotics for 2 weeks.

Cefdinir was dissolved in phosphate buffered salts at a daily gavage dose of 125 bacterial mg/kg in 2 gavages, and the probiotic bacterial solution was prepared by lyophilized bacterial powder dissolved in sterile saline at a daily gavage dose of 3×10^9 CFU in 2 gavages. Fecal and blood samples were collected on days 0, 7, 14 and 21, respectively, and stored in a refrigerator at −80 ℃.

2.4. Experimental methods

2.4.1. Laboratory animals and housing conditions

SPF grade male SD rats weighing 180–210 g were purchased from Beijing Viton Lihua Laboratory Animal Technology Co. The rats were housed in wire mesh cages in an air-conditioned room with a temperature of 23 ℃ ± 2 ℃, a relative humidity of 50%–60%, and a day-night alternation of 12 h. During the rearing period, rats were free to drink water and consume food. Drinking water was changed every 3 days, and the feed was standard commercial rodent feed containing 20% protein, 5.0% lipid and 5.0% fiber. Animal experiments were performed in accordance with the Guide for the Care and Use of Laboratory Animals and approved by the Animal Research Ethics Committee.

2.4.2. Criteria for determining intestinal dysbiosis

It has been reported that the decrease of Bifidobacterium and Lactobacillus, while the decrease of Enterobacteriaceae and Enterococcus is not or is lower than that of Bifidobacterium and Lactobacillus as the criterion of disproportion. At the same time, the modeling was considered successful when the mouse had loose feces, lazy activity, and a lack of luster in its fur.

2.4.3. Extraction of fecal macrogenomic DNA

The treatment of the rat manure: the stool samples that will be stored in the −80 ℃ refrigerator, each of which is took about 500 mg samples, and added four times the volume of the methanol in 4 ℃, and sample is mashed. Low temperature ultrasonic 20 min, vortex 3 min. Under 4 ℃, centrifugal 10 min at the speed of 12,000 rpm. Collect the clear liquid and filter under the 0.22 m organic filter.

The acquisition and processing of human feces: volunteers are asked to collect fresh feces from the sample box at the same time (the same day). From the sample box, take 0.8 g stool samples and use a sterile saline (0.90%, w/v) to dilute the fresh stool samples of each volunteer and fully shake them. Make 10%, w/v's fecal slurry. Then the fecal slurry is centrifuged at (500 g, 5 min) and the overhead suspension.

Microbial DNA was extracted by cetyltrimethylammonium bromide (CTAB) method as follows:

(1) Add 1000 μL CTAB lysate preheated in a 65°C water bath to the cellular precipitate of the pretreated fecal sample and mix well.

(2) Add 10 μL polyvinylpyrrolidone and mix well.

(3) Add 30 μL β-mercaptoethanol and mix well.

(4) Water bath at 60 ℃ for 2 h, during which the samples were inverted and mixed several times to allow the samples to be fully cleaved.

(5) Centrifuge at 15,000 rpm for 15 min, transfer the supernatant and add an equal volume of chloroform: isoamyl alcohol (25:1,v/v), centrifuge at 15,000 rpm for 15 min.

(6) After transferring the supernatant, add an equal volume of chloroform and centrifuge at 15,000 rpm for 15 min at 4 ℃.

(7) After transferring the supernatant, add 2 times the volume of ice-cold anhydrous ethanol, and centrifuge at 15,000 rpm for 15 min after standing at −20 ℃ for 30 min.

(8) Remove the supernatant completely and wash the DNA precipitate with 50% ice-cold ethanol.

(9) Dry at room temperature and reconstitute in 50 μL sterile ultrapure water containing RNase (20 μg/μL).

(10) Incubate at 35 °C for 30 min, then store at −80 °C.

2.4.4. DNA sample testing

The DNA samples used in this study were assayed by:

(1) Initial detection and quantification by agarose gel electrophoresis.

(2) Agarose gel electrophoresis to analyze the purity and integrity of DNA.

(3) Nanodrop to detect the purity of DNA (OD 260/280 ratio).

(4) Qubit 2.0 for precise quantification of DNA concentration.

2.4.5. Library construction and on-line sequencing

Each sample is about 5 μg Test-qualified DNA for library construction. The tested DNA samples were interrupted into fragments of about 350bp, and then the whole library preparation was completed by end repair, addition of A-tail, addition of sequencing junction, purification, PCR amplification and other steps. After the libraries were tested, the different libraries were mixed according to, the effective concentration and the target downstream data volume required and then sequenced using the IlluminaHiseq PE150 strategy. Each sample generated about 5Gb of data, and the raw sequencing data was uploaded to the NCBI Sequence Read Archive (SRA) database.

2.4.6. Sequence analysis

Raw off-board data were QC'd using KneadData. KneadData integrates multiple QC tools such as FastQC and Trimmomatic. First, low quality and less than 100bp read length sequences were filtered out and the removed low quality and less than 100bp sequences were matched to the murine genome (c57 mouse) using bowtie26 to remove host contamination. The remaining high quality sequences were imported into MetaPhlAn2 for microbial taxonomic analysis.

2.4.7. Resistance gene testing

Raw sequenced sequences were matched to antibiotic genes in the ARG-Annot database using GROOT to obtain a resistance poo for each sample. For the resistance genes that were considered major after matching, the sequences containing antibiotic resistance genes (ARGs) were reconstructed by MetaCherchant. At the same time, mobile elements carrying ARGs in the bacterial genome were reconstructed again. Finally, species attribution of all ARGs was finalized by Kraken and its database.

2.4.8. Statistical analysis

Differential strain comparisons between multiple groups in this study were based on a two-sided unpaired Kruskal-Wallis rank sum test ($p < 0.05$). α and β Diversity indices were generated by QIIME software. Macrogenomic pathway analyses were performed using the MetaCyc database with the threshold set at an e value of $< 10^{-4}$.

The Kruskal-Wallis test is a method of using wilcoxon rank and inspection to be generalized to various tests by two different kinds of testing, which is a non-parametric method for the analysis of single factor variance analysis. The Kruskal-Wallis test is used for multiple samples between different samples, so it is applicable to the discussion of multiple group results in this paper.

Linear discriminant analysis (LDA) and effect size (LEfSe) analyses and t-tests transformed by central logarithmic ratio (CLR) were performed to analyze intergroup differences in the macrogenomic data. The threshold for the LDA effect size was set at 2, and the CLR transformation is a popular method to address the limitations of microbial composition data. Microbial relative abundance $X_{ij}^{(k)}$ transformed by CLR was $Z_{ij}^{(k)}$ formulated as:

$$Z_{ij}^{(k)} = \log\left(\frac{X_{ij}^{(k)}}{(\prod_{j=1}^{p} X_{ij}^{(k)})^{1/p}}\right), i = 1,\ldots,n^k,\ j = 1,\ldots,p,\ k = 1,2 \quad (1)$$

To avoid zero relative abundance in the equations, the zero abundance value was replaced with the pseudo number 1×10^{-5} before performing the relative abundance normalization and CLR transformation.

The LDA is mapped to the corresponding tag space by mapping the raw data to the corresponding tag space, implementing the feature selection and the descending dimension. LDA uses the label informatics to distinguish the projection, which can significantly expand the spacing of the class, reduce the distance of the class, and improve the classification accuracy. In this article, the method can effectively amplify the difference between microbial correlation data.

3. Results and analysis

3.1. Effect of β-glucansomes on the microbial metabolome

3.1.1. Analysis of potential biomarkers

In order to identify whether the oat β-glucan fermentation process is accompanied by other metabolic changes in addition to the generation of SCFAs, the mouse fecal microbial fermentation samples were next analyzed by UPLC-QTOF-MS and 378 valid peaks were obtained in the positive ion mode. The obtained effective peak dataset was analyzed by PCA and OPLS-DA, and the results are shown in **Figure 1**. The PCA score plot based on the UPLC-QTOF-MS dataset showed a clear separation between the different treatment groups with a total variance of 83.1% (PC1 = 66.7%, PC2 = 16.4%), a plot satisfaction value of 0.889 (R^2X) for the X variables, and a prediction accuracy of 0.554 (Q^2) (**Figure 1A**).The OPLS-DA score plot showed similar results to the PCA score plot with a similar statistical pattern of sample distribution, with a total variance of 84.8% (PLS1 = 64.7%, PLS2 = 20.1%), a PLOT satisfaction value of 0.938 (R^2X) for the X variables, and a prediction accuracy of 1 (Q^2) (**Figure 1B**).

Multivariate analysis combined with univariate analysis was used to evaluate differences between sample groups. The VIP analysis based on OPLS-DA was done first, and metabolites with VIP > 1 were potential biomarkers (green for VIP > 1) (**Figure 1C**). In addition, *t*-test ($p < 0.05$) and fold change (FC > 1.2 or < 0.85) were used to further screen the components of intergroup differences (**Figure 1D**). In summary, a total of 54 variables with significant differences between groups were obtained, indicating metabolic markers characterized by higher confidence between groups.

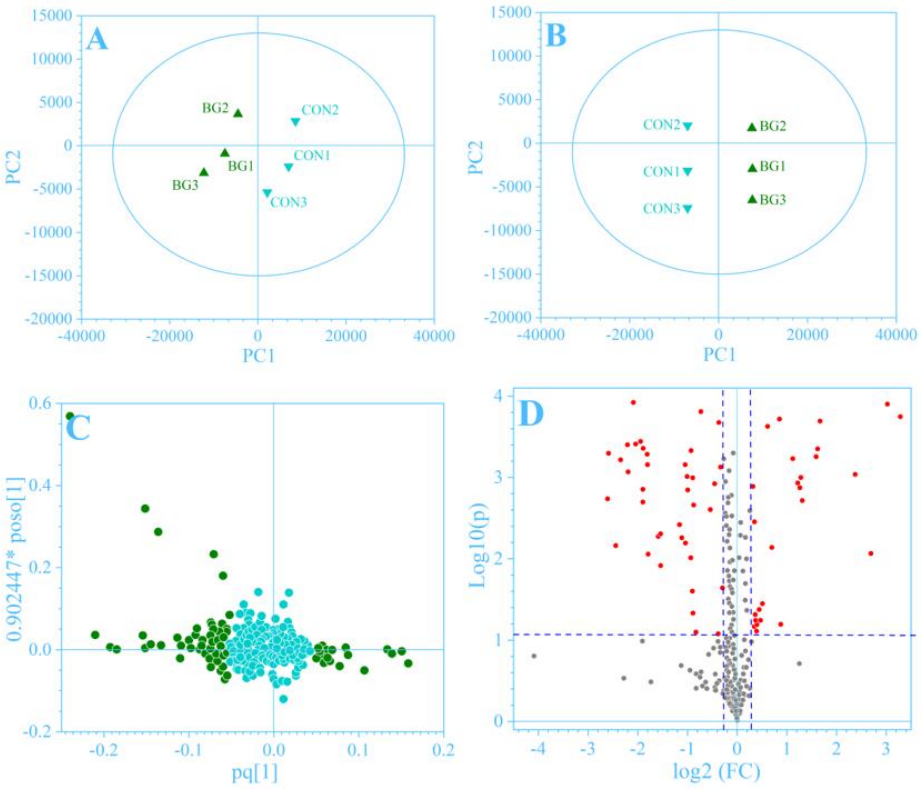

Figure 1. The effect of oat *β*-glucan fermentation on intestinal microbial metabolic profiles from mice: **(A)** PCA score plot; **(B)** OPLS-DA score plot; **(C)** The loading plot based on OPLS-DA; **(D)** The volcano plot that is used to visualize differences between groups.

In order to identify the metabolites associated with *β*-glucan fermentation, Spearman's correlation analysis was performed to analyze the relationship between gut microorganisms and metabolites, and the results are shown in **Figure 2**. As can be seen from the figure, all 54 metabolic biomarkers and 35 of the *β*-glucan fermentation-enriched microbial genera were significantly correlated ($|R| > 0.5$, $p < 0.05$), suggesting that these metabolic biomarkers are metabolic by-products produced by microorganisms during *β*-glucan fermentation.

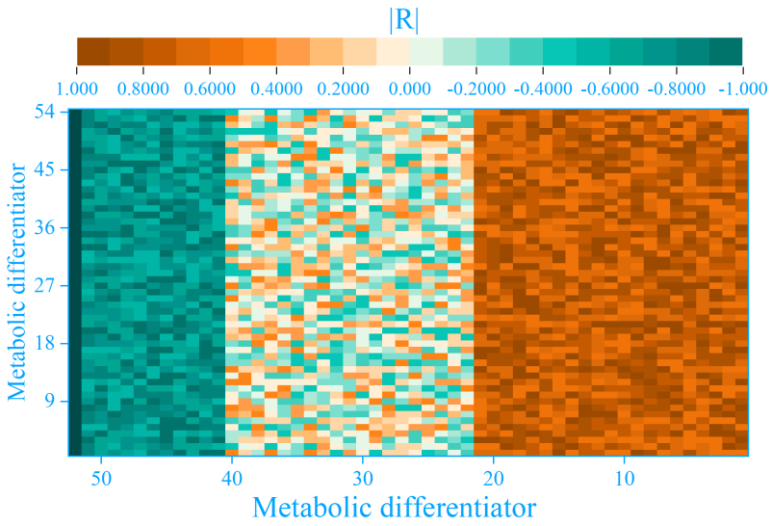

Figure 2. Analysis of the relationship between intestinal microbes and metabolites.

3.1.2. Isolation and characterization of microorganisms from the mouse gut

Fresh fecal samples were collected from healthy mice to prepare bacterial suspensions, which were coated onto GMM solid plates containing *β*-glucan as the only carbon source after gradient dilution, and the colonies were picked, separated by scribing, purified, and verified by nucleic acid electrophoresis and 16S rRNA identification. The results of the 16S rRNA identifications were as shown in **Table 3**, which showed that a total of 72 strains of intestinal bacteria that could utilize *β*-glucan were obtained, including 10 species and 4 genera (number ≥ 2), numbered Mic01–Mic10. Among them, 72 strains of Lactobacillus spp. were the main *β*-glucan metabolizing intestinal microorganisms in mice. All of the isolated Lactobacillus spp. were Lactobacillus rhamnosus, suggesting that Lactobacillus rhamnosus may be the microorganism that mainly utilizes *β*-glucan in the mouse intestine.

Table 3. Identification of isolated oat *β*-glucan-metabolizing microbes from healthy mice feces.

ID	Strain	Matching result	Score (%)	Entry number	Quantity
1	Mic01	Proteus vulgaris VBE35	100	MG027634.1	1
2	Mic02	Staphylococcus sp. BF32-10	100	MN314867.1	1
3	Mic03	Staphylococcus epidermidis R2-11-3	100	MK425675.1	1
4	Mic04	Staphylococcus sciuri sec	100	MN750602.1	1
5	Mic05	Enterobacter ludwigii R6-346-1	99.89	JQ659806.1	1
6	Mic06	Lactobacillus murinus ALB-6 gene	99.89	LC511018.1	32
7	Mic07	Lactobacillus murinus 700	100	MT585453.1	20
8	Mic08	Lactobacillus murinus TCD6	100	MH496645.1	2
9	Mic09	Lactobacillus murinus LM-B57	100	KY007190.1	12
10	Mic10	Staphylococcus sciuri NC33	99.89	MT214242.1	1
Total					72

3.1.3. Isolation and identification of microorganisms from the human gut

Anabaena spp. are the main human gut microorganisms that utilize β-glucan. In order to isolate the β-glucan-utilizing B. pseudomallei, fresh fecal samples from healthy individuals were collected to prepare bacterial suspensions, which were gradient diluted and then spread onto GMM solid plates containing β-glucan as the sole carbon source, and the colonies were picked, streaked, isolated, purified, and verified, and then subjected to nucleic acid electrophoresis and 16S rRNA identification. As a result, it was found that there was no Anabaena species among the microorganisms isolated, and it was hypothesized that this might be because Anabaena grows under more stringent conditions and could not be purified by ordinary methods for screening intestinal microorganisms. Therefore, the screening isolation was carried out by using Bacteroides-specific screening medium, and then the colonies were picked, delineated, purified, and then subjected to nucleic acid electrophoresis and 16S rRNA identification. Validation with Bacteroides-specific primers proved that the screened intestinal bacteria were basically Bacteroides.

The results of 16S rRNA identification are shown in **Table 4**, a total of 24 strains of human gut bacteria were obtained, including 10 species and 2 genera, numbered Bac01-Bac10. Among them, there were 21 strains of the genus Anabaena, including 12 strains of Bacteroides vulgatus, 2 strains of Bacteroides xylanisolvens, Bacteroides massiliensis 1 strain, Bacteroides koreensis 1 strain, Bacteroides uniformis 2 strains, and Bacteroides caccae 3 strains. In addition, 3 strains of the genus Parabacteroides, all Parabacteroides distasonis (Bac07).

Table 4. Identification of Bacteroides strains isolated from healthy adult feces.

ID	Strain	Matching result	Score (%)	Entry number	Quantity
1	Bac01	Bacteroides vulgatus D2_Ch2_95	99.92	MN081729.1	4
2	Bac02	Bacteroides xylanisolvens H207	100	JQ607746.1	2
3	Bac03	Bacteroides vulgatus W05002A	99.92	KP944149.1	1
4	Bac04	Bacteroides vulgatus 6435	99.78	MT515874.1	3
5	Bac05	Bacteroides vulgatus 6658	99.78	MT515977.1	4
6	Bac06	Bacteroides massiliensis EG4-8-2	99.72	AB200226.1	1
7	Bac07	Parabacteroides distasonis 759	99.43	CP054012.1	3
8	Bac08	Bacteroides koreensis YS-aM39	99.94	NR159117.1	1
9	Bac09	Bacteroides uniformis W19003B	99.78	KP944145.1	2
10	Bac10	Bacteroides caccae 9-P-D5-96	99.78	MT902963.1	3
Total					24

3.2. Diversity analysis of microbial composition in intestinal diseases

3.2.1. Identification of relevant markers

In order to avoid the influence of differences in confounding factors in the process of biomarker identification, the study in this paper conducted Wilcoxon rank-sum test for age and BMI and chi-square test for gender for the disease and control groups in each dataset, and the *P*-value results of the test are shown in **Table 5**. It can be seen that different intestinal diseases were not correlated with gender, six intestinal diseases

were significantly correlated with age, and one intestinal disease was correlated with BMI. The * indicates significant correlation.

Table 5. A list of *P*-values as statistical results of confounding factors**.**

Datasets	Age	BMI	Gender
PRJEB10112	0.006974*	0.117524	0.805024
PRJEB12050	0.734123	0.628012	1
PRJEB21805	0.005086*	0.683014	0.974465
PRJDB4207	0.061782	0.414382	0.820824
PRJEB6080	0.007444*	0.050121	0.316272
PRJEB7848	0.616313	0.120562	1
PRJNA427545_cohort1	0.131502	0.980224	0.098046
PRJNA375270_CD	0.964478	NA	0.974480
PRJNA405050_CD	0.012186*	NA	NA
SRP059084	NA	NA	NA
PRJNA341350_UC	0.448041	NA	0.784498
PRJNA400082_UC	0.012437*	NA	NA
PRJEB1870	8.71×10^{-12}*	3.41×10^{-9}*	0.308842

Subsequently, the *R* package "Maaslin2" was used to correct for significantly different covariates and to identify the strains and metabolic pathways associated with the disease in each dataset, where strains and metabolic pathways with a *P*-value of < 0.05 were considered to be the significantly different strains and metabolic pathways in the dataset.

Considering the heterogeneity among different datasets, in this study, we conducted a meta-analysis using the *R* language package "MMUPHin" to integrate the correlation coefficients of microorganisms and metabolic pathways with diseases in different datasets of the same disease. The *P*-values obtained from the meta-analysis were corrected using the FDR method, and the microbes and metabolic pathways with FDR < 0.05 were used as the final biomarkers for the disease.

3.2.2. Distribution of intestinal disease marker microorganisms

In order to investigate whether these disease-enriched microorganisms exhibit characteristic prevalence patterns in their respective diseases, this study constructed a binary matrix with 1 s and 0 s to indicate the presence or absence of a particular microorganism in the diseased samples, and computed the Jaccard similarity between the microorganisms to observe the co-occurrence of members of different microbial clusters in the diseased samples.

The co-occurrence and prevalence of disease-enriched microbial clusters are shown in **Figure 3**, where **Figure 3A** Co-occurrence of disease-enriched microbes in cases. The four microbial clusters (Ulcerative Colitis-specific UC, Crohn's Disease-specific CD, Colorectal Cancer-specific CRC, and Disease Shared Cluster Common-enriched) represent the Jaccard similarity between members of their respective clusters, while the background group represents the Jaccard similarity between members of the non-identical clusters, and higher Jaccard similarity indicates higher co-occurrence of

members of that cluster. The higher the Jaccard similarity, the higher the co-occurrence of the members of the group. **Figure 3B** shows the prevalence of each disease-enriched microbial cluster in different diseases. The * sign indicates that the microbial cluster was more prevalent in the case group of the corresponding disease compared to the corresponding control (statistical significance, ns, $P \geq 0.05$; *, $P < 0.05$; **, $P < 0.01$; ***, $P < 0.001$; ****, $P < 0.0001$). In the patient samples, members of the Crohn's disease and colorectal cancer-specific clusters as well as the flora of the disease-shared clusters all showed higher internal Jaccard similarity compared to the background data (Wilcoxon rank-sum test, $P < 0.0001$), suggesting that they tended to be more likely to coexist with members of the same cluster. However, ulcerative colitis-specific clusters did not show this trend.

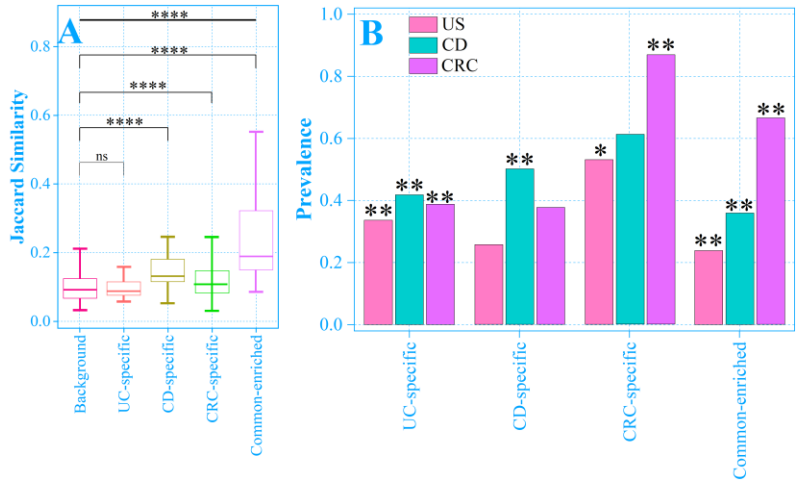

Figure 3. Co-occurrence and prevalence of disease-enriched microbial clusters: **(A)** Co-occurrence of disease-enriched microorganisms in cases; **(B)** Enrichment of the prevalence of microbial clusters in different diseases for each disease.

Next, the prevalence of these clusters as a whole was investigated across diseases. This paper found that Crohn's disease-specific clusters were significantly enriched only in patients with Crohn's disease, whereas microorganisms from disease-shared clusters were significantly enriched in patients with data from each disease. Although members of the ulcerative colitis-specific cluster lacked significant co-occurrence with each other, their prevalence was significantly higher in patients with all three diseases than in the corresponding control samples. These results suggest that it is difficult to distinguish between different intestinal diseases based solely on the prevalence of disease-enriched microorganisms.

3.2.3. Interaction of intestinal disease-marking microorganisms in different states of the body

Considering the difficulty of comparing the networks as a whole, this section of the paper examines module identification of the constructed networks using the mcode tool in Cytoscape software. The modules identified in the control and disease group networks for colorectal cancer, Crohn's disease and ulcerative colitis are shown in **Figure 4**. The node color indicates the trend of the microorganism in the disease and the node size indicates the prevalence of the microorganism in all the controls/cases of a given dataset. Gray edges (correlations) indicate positive correlations and red

edges indicate negative correlations. The thickness of the edges indicates the strength of the correlation. Modules are considered to be highly interconnected clusters in a network and are often used for biological interpretation of the network. In the colorectal cancer network, a tightly connected module ("CRC-Case1") was obtained from the disease group network, compared with 2 modules obtained from the control network ("CRC-CTR1" and "CRC-CTR2") with more members and tighter internal associations (**Figure 4A**). Microorganisms of the same genus are often more closely connected to each other, possibly because they share similar metabolic traits. The identified modules also revealed previously known positive correlations. F. nucleatum, a widely studied oral-associated anaerobic microorganism, can synergize with other anaerobic microorganisms to form biofilms and promote intestinal tumorigenesis. F. nucleatum was found to be positively correlated with P. micra in the Disease Module for colorectal cancer, which is also consistent with previous findings. Negative correlation associations were also found between species positively correlated with F. nucleatum, suggesting a possible competitive relationship between different microorganisms during biofilm formation, although these new associations remain to be verified by further experiments.

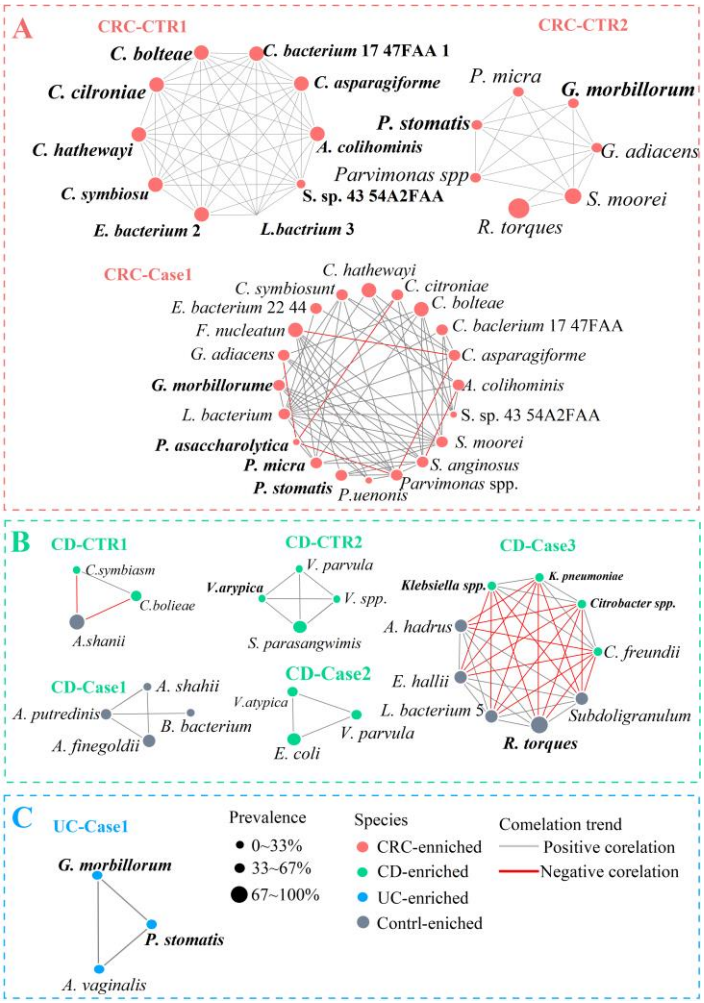

Figure 4. Detected modules from the control networks and case networks of CRC, CD and UC: **(A)** Colorectal cancer (CRC); **(B)** Crohn's disease (CD); **(C)** Ulcerative colitis (UC).

Similar to the colorectal cancer module, in the Crohn's disease dataset, compared to the control module ("CD-CTR1" and "CD-CTR2"), the disease group modules ("CD-Case1", "CD-Case2" and "CD-Case3") possessed closer interconnections between microorganisms including those belonging to the genera Alistipes, Klebsiella (Klebsiella), and Veillonella microorganisms (**Figure 4B**). In the Crohn's disease module, Klebsiella spp. and Klebsiella pneumoniae were negatively correlated with R. torques, which may be one of the patterns of interactions resulting from the inflammatory environment of the gut. In the ulcerative colitis data, only the disease group network recognized the module ("UC-Case1") (**Figure 4C**). Interestingly, a strong correlation between G. morbillorum and P. stomatis was found in both the colorectal cancer module and the ulcerative colitis module, suggesting strong synergistic effects between them.

4. Results and discussion

Gastrointestinal microorganisms play a crucial role in host health and disease and can influence the body's nutrient metabolism, immune response, and disease defense and control. Clostridium perfringens spores readily enter the gastrointestinal tract from the environment through the oral cavity and can occupy a wide range of ecological niches in the gut. Normal intestinal microflora and their metabolites can inhibit the germination and further colonization of C. perfringens spores by competing for ecological niches and nutrients and by strengthening the epithelial barrier. When the intestinal flora is dysbiotic, the conversion of primary bile acids to secondary bile acids is restricted, the concentration of primary bile acids increases, which is favorable for Clostridium spore germination, and there are not enough secondary bile acids to inhibit Clostridium spore germination and the growth of nutrients. The reduction in commensal probiotics leads to a reduction in the mucus layer, making it easier for C. perfringens to reach the intestinal epithelium and reducing intestinal barrier integrity. This leads to uncontrolled growth of Clostridium perfringens, production of toxins, and pathogenesis of the organism. β-Glucan treatment leads to changes in the gut microbial community, and the Lactobacillus spp. strains of gut microbes can provide some detoxification of β-glucan. Thus, the interaction between gut microbes and β-glucan is twofold.

The β-glucan treatment led to changes in the diversity of the gut microbial community, with α diversity decreasing and β diversity increasing. α The decrease in diversity may be due to the fact that β-glucan can inhibit the growth of certain microorganisms, whereas the changes in the overall community structure of gut microorganisms caused by β-glucan suggest that different microorganisms have different sensitivities to β-glucan. For example, microorganisms in the Lactobacillaceae family may be highly resistant to β-glucan, whereas microorganisms in the Anabacteriaceae family may be highly sensitive to β-glucan. Parthenogenetic anaerobes may be highly resistant to β-glucan and anaerobes may be highly sensitive to β-glucan. In contrast, those genera whose relative abundance is reduced by β-glucan are less resistant to β-glucan. The increased diversity may be due to the reduction of species in the gut microorganisms of the β-glucan-treated group, resulting in an increased degree of variation among individuals. α Decreased diversity has correlation

with intestinal diseases such as Crohn's disease, ulcerative colitis, viral diarrhea, eczema, and allergic diseases. The *β*-glucan can effectively promote the self-repair of the intestinal micromicrobe structure and enhance the corresponding function. This is of great significance to the theory of intestinal disease and the research of clinical treatment. At the same time, from the perspective of social ethics, the study can fully guarantee the privacy of the patients in clinical trials and to promote the fairness of the drug.

This chapter investigates the role of gut microorganisms in the regulation of intestinal diseases by *β*-glucan and reveals the potential mechanisms by which *β*-glucan alleviates colonic diseases. The main conclusions are as follows:

(1) Among the metabolites produced by Lactobacillus enterica metabolizing *β*-glucan, *L. murinus Mic07* metabolite significantly promoted LPS-induced macrophage inflammation, *L. murinus Mic08* metabolite significantly inhibited LPS-induced macrophage inflammation, and *L. murinus Mic06* and *L. murinus Mic09* metabolites had no significant effect on LPS induced macrophage inflammation without significant effects. Metabolites produced by human L. intestinalis metabolizing *β*-glucan all significantly inhibited LPS-induced macrophage inflammation.

(2) Daily gavage of *β*-glucan at a dose of 3×10^9 CFU significantly ameliorated clinical signs of enteritis, colonic tissue injury, apoptosis and inflammatory activation of colonic tissue in mice with colonic inflammation. In addition, *β*-glucan could modulate the colonic mucosal barrier function, promote the integrity of the intestinal barrier, and induce changes in the structure of the intestinal microbial community.

(3) *β*-Glucan can significantly increase the levels of SCFAs, especially acetic acid, propionic acid, and butyric acid, in the intestine, while inducing changes in the intestinal metabolic profile and metabolic pathways.

The above study does prove the important application value of microbial groups in the treatment of intestinal diseases, but in the latter studies, there is still enough Angle to further improve the study:

(1) From the perspective of system biology, the interaction network and feedback mechanism between intestinal microorganism and host are further explained.

(2) The effects of individual differences on microbial and drug reactions were fully considered, and the individual samples of different genetic backgrounds, lifestyle and disease were included in the experimental control.

(3) By using machine learning and artificial intelligence technology, it is better to predict the high dimensional data of the microbial community, and effectively predict the reaction of different individuals, and the results of the experiment are confirmed.

Ethical approval: Not applicable.

Conflict of interest: The author declares no conflict of interest.

References

1. Xu, H., Liu, M., Cao, J., Li, X., Fan, D., Xia, Y., ... & Zhao, H. (2019). The dynamic interplay between the gut microbiota and autoimmune diseases. Journal of immunology research, 2019(1), 7546047.

2. Zhang, J., Zhang, J., & Wang, R. (2018). Gut microbiota modulates drug pharmacokinetics. Drug metabolism reviews, 50(3), 357-368.
3. Zhang, X., Han, Y., Huang, W., Jin, M., & Gao, Z. (2021). The influence of the gut microbiota on the bioavailability of oral drugs. Acta Pharmaceutica Sinica B, 11(7), 1789-1812.
4. Lindell, A. E., Zimmermann-Kogadeeva, M., & Patil, K. R. (2022). Multimodal interactions of drugs, natural compounds and pollutants with the gut microbiota. Nature Reviews Microbiology, 20(7), 431-443.
5. Vich Vila, A., Collij, V., Sanna, S., Sinha, T., Imhann, F., Bourgonje, A. R., ... & Weersma, R. K. (2020). Impact of commonly used drugs on the composition and metabolic function of the gut microbiota. Nature communications, 11(1), 362.
6. Weersma, R. K., Zhernakova, A., & Fu, J. (2020). Interaction between drugs and the gut microbiome. Gut, 69(8), 1510-1519.
7. Wang, P. X., Deng, X. R., Zhang, C. H., & Yuan, H. J. (2020). Gut microbiota and metabolic syndrome. Chinese Medical Journal, 133
8. Jackson, M. A., Verdi, S., Maxan, M. E., Shin, C. M., Zierer, J., Bowyer, R. C., ... & Steves, C. J. (2018). Gut microbiota associations with common diseases and prescription medications in a population-based cohort. Nature communications, 9(1), 2655.
9. Mousa, S., Sarfraz, M., & Mousa, W. K. (2023). The interplay between gut microbiota and oral medications and its impact on advancing precision medicine. Metabolites, 13(5), 674.
10. Koppel, N., Maini Rekdal, V., & Balskus, E. P. (2017). Chemical transformation of xenobiotics by the human gut microbiota. Science, 356(6344), eaag2770.
11. Wilson, I. D., & Nicholson, J. K. (2017). Gut microbiome interactions with drug metabolism, efficacy, and toxicity. Translational Research, 179, 204-222.
12. Fan, Y., & Pedersen, O. (2021). Gut microbiota in human metabolic health and disease. Nature Reviews Microbiology, 19(1), 55-71.
13. Adak, A., & Khan, M. R. (2019). An insight into gut microbiota and its functionalities. Cellular and Molecular Life Sciences, 76, 473-493.
14. Dey, P. (2019). Gut microbiota in phytopharmacology: A comprehensive overview of concepts, reciprocal interactions, biotransformations and mode of actions. Pharmacological research, 147, 104367.
15. Cheng, L., Qi, C., Zhuang, H., Fu, T., & Zhang, X. (2020). gutMDisorder: a comprehensive database for dysbiosis of the gut microbiota in disorders and interventions. Nucleic acids research, 48(D1), D554-D560.
16. Liu, J., Tan, Y., Cheng, H., Zhang, D., Feng, W., & Peng, C. (2022). Functions of gut microbiota metabolites, current status and future perspectives. Aging and disease, 13(4), 1106.
17. Qiu, P., Ishimoto, T., Fu, L., Zhang, J., Zhang, Z., & Liu, Y. (2022). The gut microbiota in inflammatory bowel disease. Frontiers in cellular and infection microbiology, 12, 733992.
18. Le Bastard, Q., Al-Ghalith, G. A., Grégoire, M., Chapelet, G., Javaudin, F., Dailly, E., ... & Montassier, E. (2018). Systematic review: human gut dysbiosis induced by non-antibiotic prescription medications. Alimentary pharmacology & therapeutics, 47(3), 332-345.
19. ÁlvarezMercado Ana I. & PlazaDiaz Julio. (2022). Dietary Polysaccharides as Modulators of the Gut Microbiota Ecosystem: An Update on Their Impact on Health. Nutrients(19),4116-4116.
20. Jina Ha, Jinwoo Kim, Seongok Kim, Kwang Jun Lee & Hakdong Shin. (2024). Garlic-Induced Enhancement of Bifidobacterium: Enterotype-Specific Modulation of Gut Microbiota and Probiotic Populations. Microorganisms(10),1971-1971.
21. Dahiya Divakar & Nigam Poonam Singh. (2023). Antibiotic-Therapy-Induced Gut Dysbiosis Affecting Gut Microbiota—Brain Axis and Cognition: Restoration by Intake of Probiotics and Synbiotics. International Journal of Molecular Sciences(4),3074-3074.